American Journal of Pathology, Vol. 166, No. 1, January 2005

Matrix Pathobiology

Endostatin Overexpression Specifically in the Lens and Skin Leads to Cataract and Ultrastructural Alterations in Basement Membranes

Harri Elamaa,* Raija Sormunen,† Marko Rehn,* Raija Soininen,* and Taina Pihlajaniemi*

From the Department of Medical Biochemistry and Molecular Biology, Collagen Research Unit, and the Department of Pathology,† Biocenter Oulu, University of Oulu, Oulu, Finland*

Endostatin, a proteolytic fragment of type XVIII collagen, has been shown to inhibit angiogenesis, tumor growth, and endothelial cell proliferation and migration. We analyzed its functions *in vivo* by generating transgenic mice in which it was overexpressed in the skin and lens capsule under the keratin K14 promoter. Opacity of the lens occurred at 4 months of age in the mouse line J4, with the highest level of endostatin expression. The lens epithelial cells appeared to lose contact with the capsule and began to vacuolize. In 1-year-old mice the lens epithelial cell layer had entirely degenerated, and instead, large plaques of spindle-shaped cells had formed in the anterior region of the lens. Moreover, a widening of the epidermal basement membrane (BM) zone of the skin was observed in electron microscopy. The epidermal BM was conspicuously altered in the J4 mice with high transgene expression, including clear broadening and occurrence of pearl-like protrusions in some areas, whereas the BM was more even in appearance but consistently broadened in the mouse line G20 with moderate transgene expression. In both lines the BM was continuous. Measurements indicated that the lamina densa was 78.54 ± 53.10 nm in line J4, the large variation reflecting the protrusions of the lamina densa, and 44.24 ± 11.52 nm in line G20, compared with 33.74 ± 9.96 nm in wild-type adult mice. Immunoelectron microscopy of wild-type mouse skin type XVIII collagen showed a polarized orientation in the BMs, with the C-terminal endostatin region localized in the lamina densa and the N terminus in average ~40 nm more on the dermal side. Type XVIII collagen was dispersed in the transgenic skin, suggesting that the transgene-derived endostatin fragment displaces the full-length collagen XVIII. This may impair the anchoring of the lamina densa to the dermis and thereby lead to loosening of the BMs, resembling the previously observed situation in collagen XVIII-null mice. *(Am J Pathol 2005, 166:221–229)*

Type XVIII collagen, which is expressed in epithelial and endothelial basement membrane (BM) zones in a wide variety of tissues,[1,2] contains an N-terminal noncollagenous domain, an interrupted collagenous domain, and a C-terminal noncollagenous domain.[3] The most conserved region is the C-terminal endostatin domain,[4,5] a proteolytically released 20-kd fragment that strongly inhibits endothelial cell proliferation and migration, angiogenesis, and tumor growth.[6] On the other hand, the intact C-terminal noncollagenous NC1 domain containing endostatin in a trimeric form is thought to be motogenic for endothelial and nonendothelial cells.[7] α5 and αv integrins[8] and glypican can serve as receptors for endostatin.[9] Endostatin and the NC1 domain bind equally well to the extracellular matrix components fibulin-1, fibulin-2, and heparin, whereas the NC1 binds more strongly to nidogen-2 and to laminin-1.[10,11] Endostatin may also influence the wnt-pathway by affecting β-catenin stability.[12] Many proteinases are able to digest type XVIII collagen, resulting in release of the endostatin fragment, including cysteine proteinases, matrix metalloproteinases, and serine proteinases.[13–15]

Mice lacking type XVIII collagen have eye abnormalities, including delayed postnatal regression of the hyaloid vessels along the inner limiting membrane of the retina, poor outgrowth of the retinal vasculature, and impaired retinal pigment epithelial function.[16,17] They

Supported by the Finnish Centre of Excellence Programe (2000–2005) of the Academy of Finland (grant no. 44843), the Sigrid Jusélius Foundation, and the European Commission (grant QLK3-2000-00084).

Accepted for publication October 5, 2004.

Address reprint requests to Dr. Taina Pihlajaniemi, Department of Medical Biochemistry and Molecular Biology, Collagen Research Unit, Biocenter Oulu, University of Oulu, Aapistie 7, FI 90220, Oulu, Finland. E-mail: taina.pihlajaniemi@oulu.fi.

also suffer from a fragile iris and atrophy of the ciliary body.[18,19] The Knobloch syndrome, characterized by severe myopia, vitreoretinal degeneration, macular abnormalities, and occipital encephalocele, is an inherited human autosomal disorder caused by mutations in the type XVIII collagen gene.[20,21] Type XVIII collagen appears to be involved in kidney and lung epithelial bud development,[22] and the endostatin domain of type XVIII collagen in *Caenorhabditis elegans* is needed for the normal migration of cells and axon guidance.[4]

To study the biological function of the endostatin domain of type XVIII collagen, we generated transgenic mice synthesizing endostatin under the K14 promoter, which is known to direct gene expression in epidermal basal cells and lens epithelial cells.[23] Endostatin overexpression was found to markedly affect the lens and skin, leading to lens opacity and a broadened epidermal BM. The severity of the lens and skin findings correlated with the level of endostatin overexpression in independent transgenic lines. We also analyzed the location of type XVIII collagen molecules in the skin, and the resulting data enable us to propose a new model for the role of endostatin in the organization of BMs.

Materials and Methods

Generation of Transgenic Mouse Lines

A transgenic cDNA construct encoding the signal sequence and C-terminal endostatin part of the type α1(XVIII) chain was generated by polymerase chain reaction (PCR) using a mouse cDNA clone[3,24] as a template and the partially complementary primers 5′-GGATCCGGCCCAGCGCA-3′; 5′-ATGGTGATGGTGATGGTGATCAGCGCTGGCAGGCA-3′; and 5′-CACCATCACCATCACCATACTCATCAGGACTTT-3′; 5′-GGATCCTATTTGGAGAAAGAGGTCATGAAG-3′. In the second step, PCR was performed using DNA fragments from the first PCR reactions as the template and the primers 5′-GGATCCGGCCCAGCGCA-3′ and 5′-GGATCCTATTTGGAGAAAGAGGTCATGAAG-3′. The ensuing PCR fragment was digested with *Bam*HI, ligated into the K14 promoter expression cassette,[23] and the insert was injected into fertilized mouse oocytes of the strain FVB/NIH. The genotypes of the transgene mice were confirmed by Southern blotting and PCR with the specific primers 5′-GCGCAGAGGCTCTCACTGCCCTGAT-3′ and 5′-GAGATAGCACCTCGTCCTTCAGGTT-3′. *Col18a1*$^{-/-}$;K14-endostatin double-mutant mice were generated by crossbreeding the *Col18a1*$^{-/-}$[16] and the endostatin transgenic mice.

Analysis of Transgene Expression

For reverse transcriptase (RT)-PCR analysis, total RNA was isolated from whole eyes using Tri Reagent (Sigma Chemical Co., St. Louis, MO) according to the manufacturer's instructions, and reverse transcriptase reactions were performed with 2 μg of total RNA as a template and 0.5 μg of hexamers as primers. The PCR primers used were 5′-GCGCAGAGGCTCTCACTGCCCTGAT-3′ and 5′-GAGATAGCACCTCGTCCTTCAGGTT-3′.

For Western blotting of whole eye samples, protein homogenates were prepared using the Tri Reagent (Sigma Chemical Co.). The precipitated proteins were dissolved in 32 μl of 4× sodium dodecyl sulfate (SDS) sample buffer and β-mercaptoethanol was added to 5%. The skin samples were prepared by homogenizing 1-cm^2 pieces of skin in 1 ml of 8 mol/L urea, 0.5 mol/L NaCl, 20 mmol/L Tris, pH 7.9, with 2% β-mercaptoethanol using an ultra turrex homogenizer, after which the homogenates were centrifuged at 13,000 rpm for 10 minutes. Ten μl of the skin and eye supernatants with 4% SDS sample buffer were analyzed by denaturing 15% SDS-polyacrylamide gel electrophoresis followed by staining with Coomassie Brilliant Blue and Western blotting onto polyvinylidene fluoride membranes. The filters were blocked with 5% fat-free milk powder-0.1% Tween 20 in Tris-buffered saline, pH 7.4. The polyclonal antibody against endostatin, RES,[25] was used in a dilution of 0.5 μg/ml and incubated overnight at + 4°C. The reactions were detected with a horseradish peroxidase-conjugated goat anti-rabbit secondary antibody (Bio-Rad, Richmond, CA) and enhanced chemiluminescence reagents (Amersham, Arlington Heights, IL) as recommended.

For immunofluorescence stainings, frozen samples were cut into 5-μm and 9-μm cryosections and fixed in ethanol for 10 minutes at −20°C. The sections were blocked by incubation with a 1% blocking reagent (Boehringer Mannheim, Indianapolis, IN) in phosphate-buffered saline (PBS), pH 7.4, for 1 hour at room temperature followed by overnight incubation at + 4°C with an anti-mouse His-tag monoclonal antibody (34660; Qiagen, Valencia, CA) and the anti-rabbit endostatin polyclonal antibody. After thorough washing with PBS, pH 7.4, a Cy3-conjugated goat anti-rabbit antibody (Jackson Immunoresearch Laboratories Inc., West Grove, PA) was applied as the endostatin antibody and an Alexa 568-conjugated goat anti-mouse antibody (Molecular Probes, Eugene, OR) as the His-tag antibody, and the samples were incubated for 60 minutes in the dark at room temperature. After extensive washing, the slides were mounted in immu-mount (Shandon Inc., Pittsburgh, PA) and examined under an epifluorescence microscope.

For paraffin sections, the tissues were fixed in 4% paraformaldehyde, dehydrated, and embedded in paraffin and sectioned at 5 μm. Immunostainings of the paraffin sections were performed using the histomouse SP kit (Zymed, South San Francisco, CA) according to the manufacturer's instructions.

Histology

Eyes from transgenic and control mice of different ages were obtained and fixed in phosphate-buffered 4% paraformaldehyde for 24 hours. After the fixation the samples were dehydrated and transferred to the infiltration solution of the Leica Historesin embedding kit (Leica Microsystems Nüssloch GmbH, Heidelberg, Germany) for 3 days with two changes of the infiltration solution. The

samples were embedded in an embedding medium (Leica) and attached to a block holder after polymerization with the Leica Historesin mounting medium (Leica). Plastic sections (1.5 to 3 μm) were prepared and stained with hematoxylin and eosin (H&E) by routine methods.

Transmission Electron Microscopy (EM)

Skin samples from control and transgenic mice were fixed in 2.5% glutaraldehyde in 0.1 mol/L phosphate buffer, postfixed in 1% osmium tetroxide, dehydrated in acetone, and embedded in Epon Embed 812. Thin sections were cut with a Reichert Ultracut ultramicrotome and examined in a Philips CM100 transmission electron microscope. Images were captured and the thicknesses of the BMs measured by a charge-coupled device camera equipped with TCL-EM-Menu version 3 from Tietz Video and Image Processing Systems GmbH. The measurements included both the lamina lucida and the lamina densa or only the latter. Statistical analyses were performed using the *t*-test and the *F*-test, and BM/lamina densa thicknesses were analyzed in 11 transgenic and 7 wild-type mice altogether, 25 measurements for each mouse. The age of the mice varied from 2.5 months to 5.5 months.

Immunoelectron Microscopy

Skin and eye samples for immunogold labeling were isolated from the transgenic and wild-type mice, fixed in 4% paraformaldehyde in 0.1 mol/L phosphate buffer with 2.5% sucrose for 2 hours at room temperature, immersed in 2.3 mol/L sucrose, and frozen in liquid nitrogen. Thin cryosections were cut with a Leica Ultracut UCT microtome. The sections were first incubated in 0.05 mol/L glycine in PBS followed by incubation in 5% bovine serum albumin with 0.1% CWFS (cold water fish skin) gelatin in PBS. The antibodies and gold conjugate were diluted in 0.1% bovine serum albumin-C in PBS. All washings were performed in 0.1% bovine serum albumin-C in PBS. The sections were then incubated with polyclonal antibodies against endostatin, RES,[25] and against the N-terminal part of type XVIII collagen, ELQ (Saarela J, Rehn M, Vainio S, Pihlajaniemi T, unpublished), for 60 minutes, followed for 30 minutes by a protein A-gold complex. The controls were prepared by performing the labeling procedure without any primary antibody. The sections were embedded in methylcellulose and examined as described above.

Double-labeled adult wild-type skin samples were used to determine the distances of the RES (5-nm gold particles) and the ELQ (10-nm gold particles) signals from the border between the lamina lucida and the lamina densa. The analysis was performed from two wild-type mice so that random fields along the epidermal BM were assessed from both skin samples and from each field the distance of all BM-associated gold particles, ELQ (n = 111) and RES (n = 115), were measured. Statistical analyses were performed using the *t*-test and the *F*-test, and SD was calculated for the values.

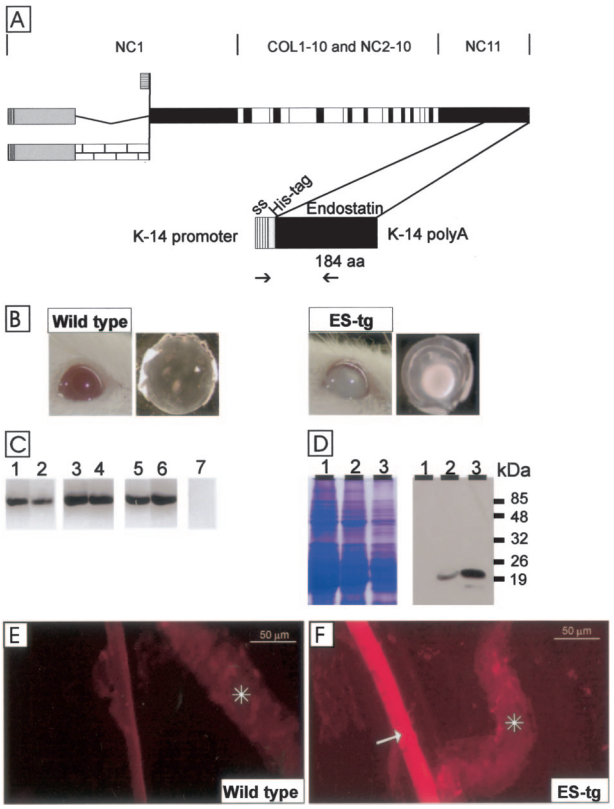

Figure 1. A: Polypeptide structures of type XVIII collagen and the transgenic endostatin construct. The **top** part shows the schematic structure of the full-length variants of the mouse α1(XVIII) chain. Collagenous sequences are shown in white, noncollagenous domains common to all variants are shown in black, noncollagenous sequences common to both long variants are shown in gray, and a noncollagenous sequence specific to the longest variant is shown with a brick pattern. The **bottom** part shows the schematic structure of the transgene product. The cDNA encoding a 184-residue endostatin sequence (aa) starting with residues HTH and preceded by a tag of six His-residues and a signal sequence (ss) was inserted between the K14 promoter and a polyA tail. The locations of the primers used for RT-PCR are indicated by **arrows**. **B:** Opacity of the lens in a 12-month-old J4 transgenic mouse (ES-tg) and a nuclear cataract in a lens dissected from a 5-month-old J4 mouse. Age-matched controls are also show. **C:** RT-PCR analysis of transgene-derived endostatin expression in whole eyes of mice of lines K18 (**lanes 1** and **2**), G20 (**lanes 3** and **4**), and J4 (**lanes 5** and **6**) at ages of 3 months (**lanes 1**, **3**, and **5**) and 8 months (**lanes 2**, **4**, and **6**) with primers specific for the transgene product. A control reaction (**lane 7**) with wild-type RNA was negative. **D:** Transgene expression in the eyes of mouse lines K18 (**lane 1**), G20 (**lane 2**), and J4 (**lane 3**) was analyzed by Western blotting (**right**). Equal loading of protein samples was verified by Coomassie staining (**left**). The anti-endostatin antibody recognized a major 20-kd fragment in 3-month-old transgenic mouse lines G20 and J4. **E** and **F:** Localization of transgenic endostatin in the lens capsule. Immunofluorescence stainings of samples from wild-type mice (**E**) and J4 mice (**F**) with the His-tag antibody. The His-tag antibody stained the whole lens capsule in the transgenic mouse, but no staining was detected in the wild-type mouse. Scale bars, 50 μm. **Asterisks**, iris.

Results

Generation of Transgenic Mice Overexpressing Endostatin

A cDNA encoding the extreme 184 C-terminal amino acid residues encompassing the endostatin domain of mouse type XVIII collagen, a signal sequence, and six histidine residues for specific detection of the transgenic protein was generated by PCR (Figure 1A). The cDNA was inserted into an expression vector with a K14 promoter,

and the plasmid was injected into fertilized oocytes to create transgenic mice lines. The transgenic mice were identified by Southern blotting and PCR (data not shown), and three independent transgenic founders, named K18, G20, and J4, were obtained. The transgenic founder mice were mated with FVB/N mice to generate separate lines and bred to homogeneity.

Transgene Expression in the Lens Leads to Opacity of the Eyes

The transgenic mice overexpressing endostatin developed a striking opacity of the eyes (Figure 1B). This became apparent at the macroscopic level at 4 to 8 months of age in line J4, and after 10 months the penetrance was nearly complete. Progressive nuclear cataract was observed in dissected lenses (Figure 1B). The macroscopic appearance of the eyes and the lenses of the G20 and K18 mice were as observed for wild-type mice (data not shown) apparently because of the lower transgene expression level found in these two lines (see below).

To analyze whether the transgene was expressed in the eyes, total RNAs were isolated from whole eyes of 3- and 8-month-old transgenic mice and RT-PCR analysis was performed using a primer pair specific to the transgene. RT-PCR products were obtained in all three transgenic mouse lines, but the signal appeared to be somewhat weaker in the K18 line (Figure 1C).

Analysis of protein extracts prepared from the eyes of 3-month-old transgenic mice by SDS-polyacrylamide gel electrophoresis and Western blotting revealed strong 20-kd signals with an anti-endostatin antibody, RES, in mice of lines G20 and J4 (Figure 1D). The transgene signal appeared to be highest in the J4 line and moderate in the G20 line, whereas it was below the detection level in the K18 line (Figure 1D).

Immunofluorescence stainings were performed using the anti-endostatin antibody, which detects both the endogenous and transgene-derived products, and an anti-His antibody that is specific to the transgene product, to study transgene expression in the eye. In the wild-type eye sections the endostatin signal was localized at the surface of the lens capsule (data not shown) as has been described previously.[16] The anti-His antibody only detects the transgene product, and staining was seen throughout the lens capsule (Figure 1, E and F). This expression pattern was observed in all three transgenic mouse lines.

Abnormalities in the Lens Epithelial Cell—Lens Capsule Zone in Endostatin Overexpression Mice

Light microscopy of plastic-embedded, H&E-stained sections from the eyes of 4-month-old mice revealed vacuoles in the lens epithelial cell layer of the transgenic mice (Figure 2, A and C). These changes were most prominent in line J4 (Figure 2C), with the highest transgene expression, but changes in the epithelial layer could also be seen in line G20, albeit to a somewhat lesser extent at this age, and an increasing number of vacuoles were observed between the epithelial cells and the lens capsule as the mice grew older (Figure 2E).

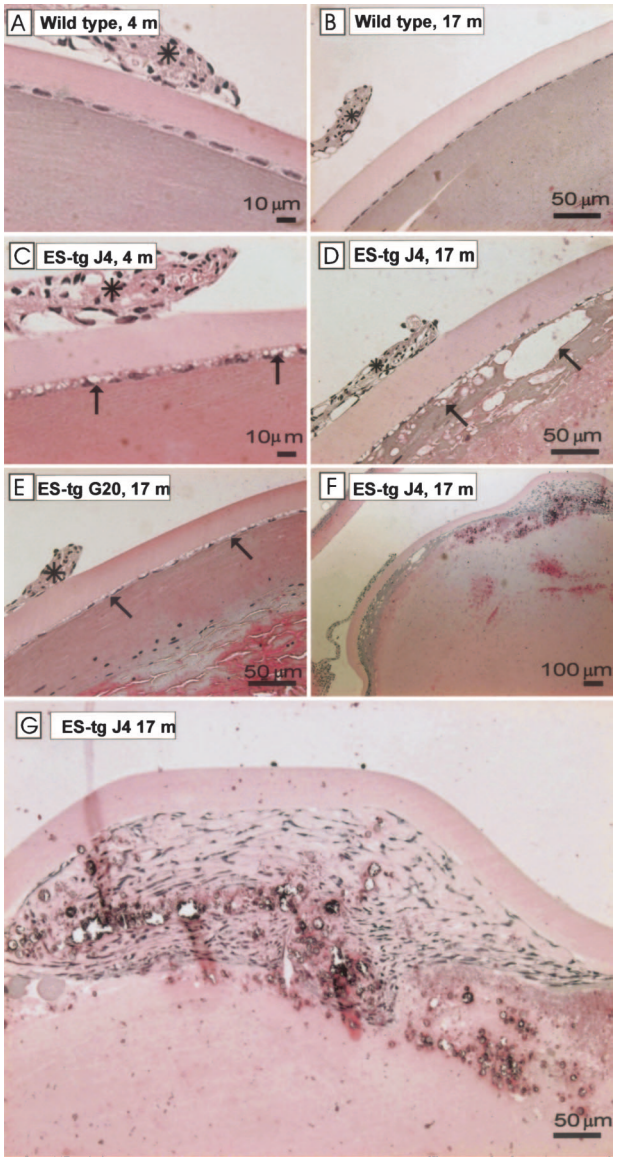

Figure 2. Histological analysis of lens capsules. H&E-stained plastic sections from 4- (**A**, **C**) and 17-month-old (**B**, **D**–G) mouse lenses representing wild-type mice (**A**, **B**) and the transgenic mouse lines J4 (**C**, **D**, **F**, **G**) and G20 (**E**). The older transgenic mouse line G20 showed increased numbers of vacuoles (**arrows**) between the lens capsule and the epithelial cells. The normal lens architecture is lost in the J4 mouse and the cortical regions of the lens show deterioration (**D**, **F**). The epithelial cell morphology is lost, and a large pile of spindle-shaped cells is formed beneath the lens capsule (**F**, **G**). The iris is indicated by a **black asterisk**.

The epithelial cell layer and the fiber cells beneath it appeared to have degenerated entirely by the time the mice reached 1 year of age (Figure 2, D and F), whereas layers of clumped cells had formed in the anterior part of the lens (Figure 2, F and G), where the cells seemed to have partly retained contact with the lens capsule. These severe defects were most readily seen in line J4. Moreover, the anterior part of the lens capsule appeared to be

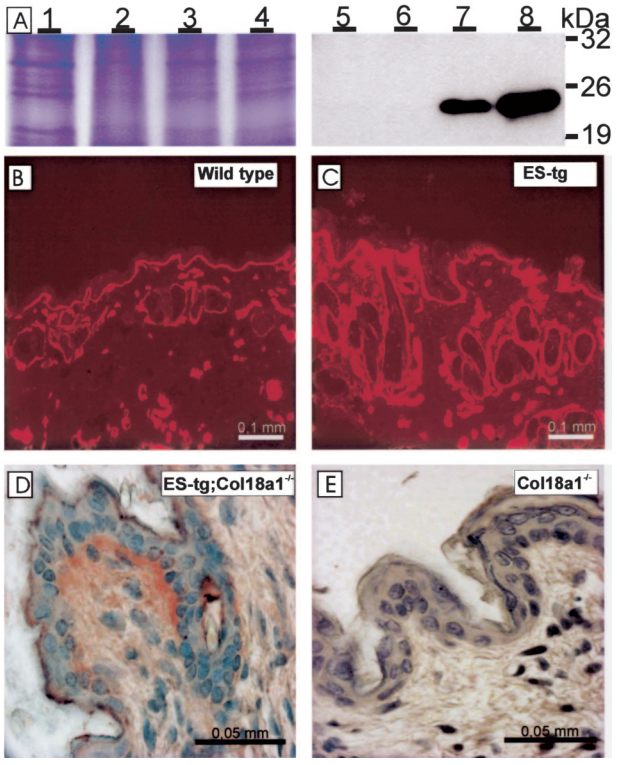

Figure 3. Analysis of the expression and localization of the transgene product in the skin. **A:** Analysis of transgenic endostatin expression in the skin of the various mouse lines by Coomassie staining (**left**) and Western blotting (**right**) of protein homogenate samples from adult mice. The skin samples are presented in the following order: wild-type mouse samples (**lanes 1** and **5**), K18 mice (**lanes 2** and **6**), G20 mice (**lanes 3** and **7**), and J4 mice (**lanes 4** and **8**). The Coomassie staining demonstrates equal loading of protein homogenates, whereas Western blotting with the RES antibody detects a fragment between the 19- and 26-kd markers in the skin samples of the G20 and J4 lines. **B** and **C:** Immunofluorescence staining of skin samples from a 2-month-old wild-type mouse (**B**) and a J4 transgenic mouse (**C**) with RES antibody. Clear staining is seen in the BM region of the epidermis-dermis junction and in the hair follicles, and this is stronger in the transgenic mouse. **D** and **E:** Immunohistological analysis of *Col18a1*$^{-/-}$ K14-endostatin (**D**) and *Col18a1*$^{-/-}$ mouse skin (**E**) with the RES antibody. Transgenic endostatin is localized in the same structures in the *Col18a1*$^{-/-}$ K14-endostatin mouse (**C**) as in the control (**B**), while the *Col18a1*$^{-/-}$ sample is negative (**E**).

thicker in the J4 line than in the control mice (Figure 2, B and D), but this was not analyzed statistically. Finally, the lens became totally atrophied. No ruptures of the lens capsule were observed.

Transgene Expression in the Skin

The ability of the K14 vector to guide expression of the transgene in the skin was confirmed by SDS-polyacrylamide gel electrophoresis fractionation and Western blotting of skin samples from 8-month-old control mice and all three transgenic mouse lines. The anti-endostatin antibody recognized a 20-kd fragment in samples from the G20 and J4 lines, whereas samples from wild-type and K18 mice were negative under these conditions (Figure 3A). The differences in the intensities of the signals corresponded to the previously noted differences in transgene expression in the eyes of the three lines (Figure 1, C and D).

Immunofluorescence staining was performed to localize the transgenic endostatin in the skin. Because the anti-His antibody gave strong background staining in the skin, the anti-endostatin antibody RES was used to detect both transgene and endogenous gene products. The immunostainings were performed on samples from 2-, 4-, and 8-month-old mice, and typical staining patterns are shown in Figure 3. In the wild-type skin the endogenous endostatin/type XVIII collagen was localized in the BM regions of the epidermis-dermis junction, the hair follicles, and the blood vessels (Figure 3B), and the same was true of the transgenic mouse skin, but the intensity of the staining was stronger (Figure 3C).

To ascertain the expression pattern of the transgene-derived endostatin, the J4 mice were mated with *Col18a1*$^{-/-}$ mice to obtain offspring lacking endogenous type XVIII collagen/endostatin expression but expressing the transgene-derived endostatin. The anti-endostatin signal was observed at the epidermal-dermal zone in these *Col18a1*$^{-/-}$;K14-endostatin mice (Figure 3D) in a manner similar to that of the endogenous endostatin signal (Figure 3B), whereas no signal was detected in the *Col18a1*$^{-/-}$ mice (Figure 3E). This indicates that the deposition of transgene-derived endostatin in the epidermal BM was comparable to that of the endogenous type XVIII collagen/endostatin. The dermal vessels were not stained, which was consistent with the K14-derived expression being restricted to the epidermis.

A Broadened Epidermal BM in Endostatin Overexpression Mice

The strong expression of the K14 promoter-derived transgene in the skin prompted a search for skin defects in the transgenic mice, but no obvious changes were observed at the light microscope level, in which the blood vessel density and general appearance of the vessels were also similar in the wild-type and transgenic mice (data not shown). At the EM level, however, we observed abnormal broadening of the epidermal BM in the J4 and G20 transgenic mice compared with the age-matched wild-type mice. More specifically, the BM was clearly broadened in the J4 mice when compared with wild-type samples (Figure 4, A and B). The BM was continuous and had an even appearance in most areas of the J4 samples but in some areas we observed pearl-like protrusions of the lamina densa (Figure 4C). Moreover, there were also regions where the lamina lucida was not detectable at all (Figure 4C). Because of the protrusions the J4 skin BM showed variability in its thickness. In G20 mice the BM was continuous and even in appearance, and it lacked the protrusions seen in J4 suggesting a milder phenotype (data not shown). However, also in G20 mice the BM was consistently broader than in control skin (Figure 4D).

The thickness of the BM (distance from the basal cell surface to the outer edge of the lamina densa) and that of the lamina densa itself were measured in 2.5-, 3.5-, and 5.5-month-old mutant and control mice, giving values of 48.90 ± 13.00 nm, 57.06 ± 15.66 nm, and 93.26 ± 62.54 nm in the control, G20, and J4 mice, respectively, for the

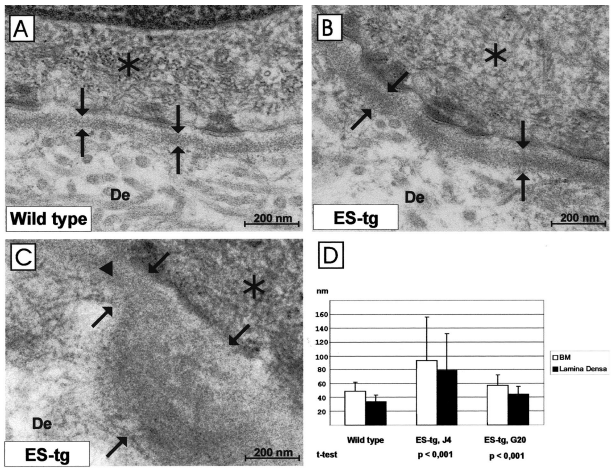

Figure 4. Ultrastructural changes in the skin BM. Transmission EM of the BM from wild-type (**A**) and transgenic J4 mice (**B**, **C**). The epidermal BM is broader in the transgenic skin (**B**, **C**) than in the wild-type skin (**A**). **D:** The thicknesses of the BM (measured from the basal cell membrane to the outer edge of the lamina densa, see **arrows** in **C**) and of the lamina densa alone (between the **arrows** in **A** and **B**) were measured in the control and transgenic mouse lines (J4 and G20) at ages between 2.5 to 5.5 months. Standard deviations are marked by **vertical bars**. Statistical significances of differences between the control and mutant samples are indicated. The detectable lamina lucida is shown by an **arrowhead**. De, dermis. **Asterisk**, Basal cell.

BM (Figure 4D), and 33.74 ± 9.96 nm, 44.24 ± 11.52 nm, and 78.54 ± 53.10 nm for the lamina densa (Figure 4D). The differences between the control and G20 samples were statistically significant in both groups ($P < 0.001$), as were those between the control and J4 samples ($P < 0.001$). Immunofluorescent staining of skin sections with antibodies against the major BM components (collagen IV, laminin β1 chain, and perlecan) did not reveal any clear differences between the mutant and control mice (data not shown).

Polarized Location of Type XVIII Collagen in the Epidermal BM

The localization of the transgenic endostatin in the same structures as endogenous type XVIII collagen in the skin raises the possibility of dominant-negative effects of transgenic endostatin. To gain an understanding of the mechanism of broadening of the epidermal BM and the role of type XVIII collagen and endostatin in this process, we performed immunolocalization of type XVIII collagen using two antibodies, the ELQ antibody against the N-terminus of type XVIII collagen and the RES antibody against the C-terminal endostatin domain. Light microscopy did not show any clear differences in immunofluorescence staining with the ELQ antibody between the control and transgenic skin samples (data not shown).

Interestingly, immunoelectron microscopy showed labeling with the RES antibody in the lamina densa of the wild-type skin (Figure 5A) and with the ELQ antibody below the lamina densa (Figure 5A). This difference in the staining patterns was originally observed when samples were labeled separately with the RES and ELQ antibodies (Figure 6, A and D). The finding was pursued further by

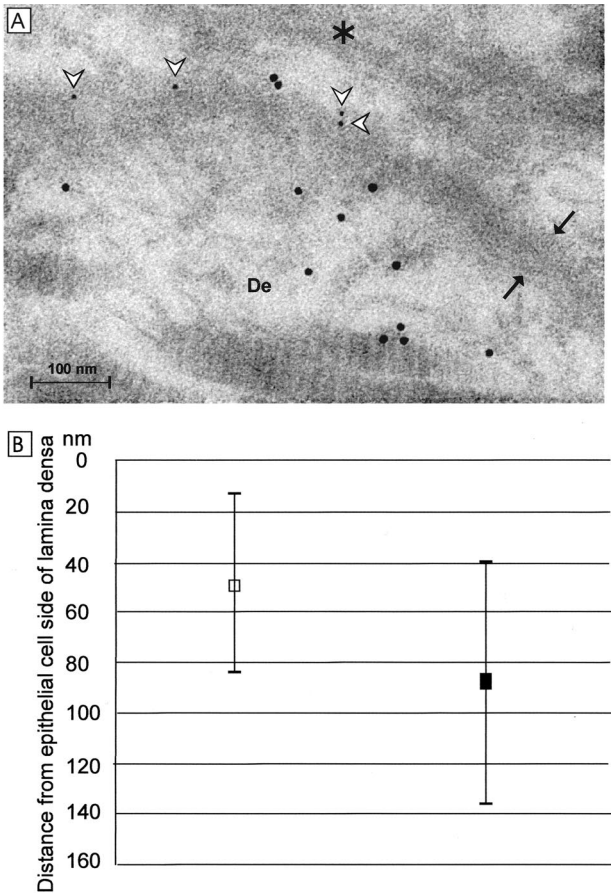

Figure 5. Type XVIII collagen has a polarized orientation in the epidermal BM. **A:** Immunoelectron microscopy of an adult mouse skin sample double labeled with the C-terminal antibody RES (**white arrowheads** pointing to 5-nm gold particles) and the N-terminal antibody ELQ (10-nm gold particles). De, Dermis. **Asterisk**, Basal cell. The lamina densa is located between the **arrows**. **B:** Measured locations of the C-terminal and N-terminal epitopes. Skin samples taken from two adult wild-type mice were double labeled with the two antibodies and measurements were performed from random fields along the epithelial BMs. The distances of the RES-associated 5-nm gold particles (**white square**, $n = 115$) and the ELQ-associated 10-nm gold particles (**black square**, $n = 111$) are shown from the epithelial edge of the lamina densa (0 nm) to the direction of the dermis. The **vertical lines** indicate the SD of the measurements. Note that the dimension of the BM is not identical in the cryoimmunoelectron microscopy sample shown here to those obtained in the case of plastic-embedded samples (see Figure 4).

double labeling of wild-type adult skin samples with the two antibodies, the results confirming the difference in the staining patterns (Figure 5A). The distances of the RES-associated small gold particles and the ELQ-associated larger gold particles from the epithelial side of the lamina densa were measured and found to be 46.80 ± 18 nm and 87.61 ± 48.61 nm, respectively, for RES and ELQ (Figure 5B). The differences in the measured distances of the two antibody signals were statistically highly significant ($P < 0.001$). This staining pattern suggests a polarized orientation of type XVIII collagen in the epidermal BM, the C-terminal part of the type XVIII collagen, endostatin, being localized in the lamina densa and the N-terminal part of the type XVIII collagen being oriented toward the dermal zone of the BM. Moreover, the two signals are separated in average by ~40 nm.

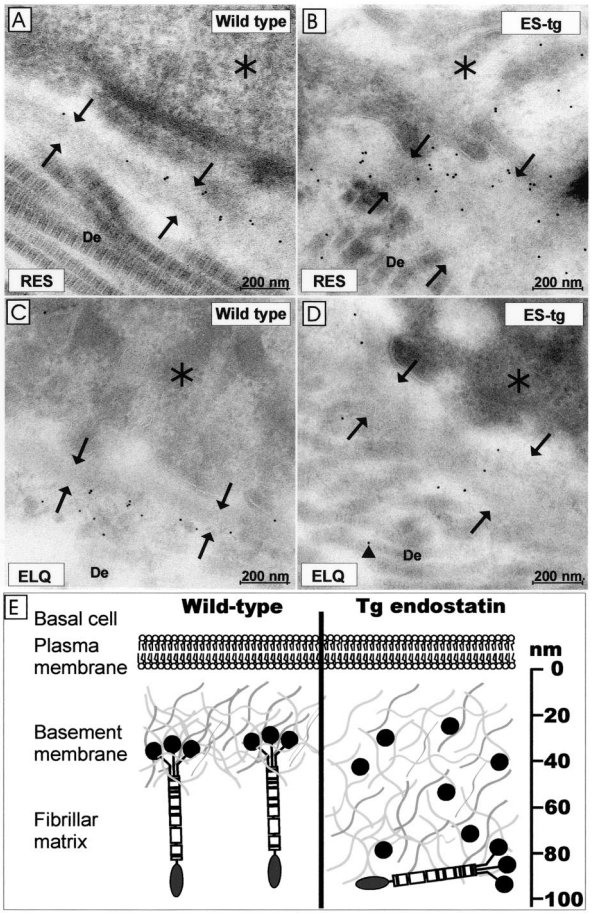

Figure 6. Localization of type XVIII collagen in the skin by immunoelectron microscopy. Samples from 5.5-month-old control (**A**, **C**) and transgenic mice (**B**, **D**) were stained with the C-terminal anti-endostatin antibody (**A**, **B**) and the N-terminal antibody ELQ (**C**, **D**). The anti-endostatin labels are located on the lamina densa of the BM (**arrows**) in the control sample and throughout the widened BM in the transgenic mouse sample. The ELQ antibody staining is located under the BM on the dermal side of the control sample but the labeling is diminished and dispersed (**arrowhead**) in the transgenic sample, indicating displacement of the endogenous type XVIII collagen. De, Dermis. **Asterisk**, Basal cell. **E:** Schematic presentation of the lack of type XVIII collagen and overexpression of endostatin in the mouse skin. Immunoelectron microscopy shows type XVIII collagen to have a polarized orientation in the BM, the endostatin-containing C-terminal end being embedded in the BM and the N-terminal domain being located at the interface of the BM and the fibrillar matrix. In view of the defects noted in the null and endostatin-overexpressing mice, we suggest that the trimeric endostatin of the full-length type XVIII collagen molecule binds to some of the BM components and tightens the BM structure. Overexpression of transgene-derived endostatin results in broadening of the BM and displacement of the endogenous type XVIII collagen to the fibrillar matrix. We propose that the monomeric endostatin competes with trimeric endostatin and thereby results in loosening of the BM molecular network. The broadening of the BMs is indicated.

Misalignment of Endogenous Type XVIII Collagen in the Epidermal BM of Endostatin Overexpression Mice

The RES antibody can be expected to react with both endogenous type XVIII collagen and transgenic endostatin in the transgenic skin, and in fact immunoelectron microscopy of the transgenic skin revealed strong but somewhat dispersed labeling, reflecting the higher endostatin level and broadened BM in endostatin overexpression mice (Figure 6B). Staining with the ELQ antibody was diminished in the transgene skin compared with the control samples (Figure 6D). Moreover, the signal pattern was typically altered, the gold label often being seen deeper in the dermis in the transgenic samples than in the control samples (Figure 6D). This staining result suggests that an excess of endostatin at least partly disturbs the localization of endogenous type XVIII collagen, causing possible disorganization and loosening of the BM.

Discussion

We generated transgenic mice overexpressing endostatin to assess the physiological role of this special C-terminal domain of type XVIII collagen. To this end, a cDNA-encoding endostatin was inserted under the keratin K14 promoter, which is known to drive expression mainly in the basal cells of the epidermis.[23] The transgenic endostatin started with residues HTH, which were identified as the N-terminal end of endostatin isolated from conditioned medium of a mouse endothelial hemangioendothelioma cell line.[6] The construct did not encode the association and hinge domains of the type XVIII collagen NC1 domain,[10] and thus led to the synthesis of monomeric endostatin. Three independent transgenic mouse lines were generated, varying in their levels of transgenic endostatin expression as shown by Western blot analysis of lens and skin samples. The weak transgene expression in line K18 did not lead to phenotypic alterations, whereas the moderate endostatin overexpression observed in line G20 and the strong expression in line J4 led in both cases to changes in the lens and the skin. The changes observed in the J4 and G20 mice were similar, although more pronounced in J4, suggesting that the observed phenotypic changes are in both lines because of the endostatin overexpression rather than to site-of-insertion differences. We conclude that the phenotypic consequences observed in the J4 and G20 reflect differences in the endostatin overexpression levels, and thus the effects appear dose-dependent.

The externally most obvious consequence of the endostatin overexpression was development of lens opacity because of progressing nuclear cataract in line J4 mice. Light microscopy revealed progressive occurrence of vacuoles in the epithelial cell layer. In the older mice the epithelial cells became spindle-shaped and formed clusters on the anterior side of the lens. This process resembled the epithelial-mesenchymal transition in the lens caused by transforming growth factor-β.[26] Microscopic changes in the lens epithelial cell layer and the lens capsule were also clearly evident in the G20 mice, but the changes occurred later than in the J4 mice and did not progress to the stage marked by opacity of the lens.

Prompted by the strong lens phenotype in the transgenic mice, we examined the expression of the transgene in the eye. One report indicates that the K14 promoter is expressed in the lens epithelium in neonates.[27] RT-PCR, Western blotting, and immunofluorescence staining all confirmed the presence of transgenic endostatin in the mouse lens. The expected 20-kd endostatin fragment was detected in eye homogenates representing

lines G20 and J4, but not in those of line K18, which had only weak RT-PCR signals. Comparison of the location of the transgenic endostatin with that of the endogenous gene product revealed both in the lens capsule, but with the transgenic form in higher amounts and more broadly distributed throughout the capsule.

The lens capsule is a specialized BM providing support for the attachment of epithelial cells,[28,29] and overexpression of endostatin in the lens appeared to lead first to loosening of the epithelial cell contact with the lens capsule and at later stages to abnormal proliferation and clustering of the cells. The capsule also appeared to be thickened. We conclude that the excess of endostatin and its abnormal localization may cause disorganization of the capsule, although it was not ruptured in the transgenic mice. Integrin $\alpha5\beta1$ has been suggested as a functional receptor for endostatin,[8,30] which in turn is known to bind to glycosaminoglycans in a specific manner,[31] including binding to the cell surface heparan sulfate proteoglycans glypicans 1 and 4.[9] Endostatin is also known to cause disassembly of the actin cytoskeleton via down-regulation of RhoA activity.[32] The oncogenes E6 and E7, which effect the cell-cycle protein p53 and the retinoblastoma protein (pRB) when expressed under the K14 promoter, cause deregulation of the cell cycle in lens epithelial cells and lead to cataract development in mice.[27] Thinking along these lines, it is of interest to note that endostatin can cause cell-cycle arrest in endothelial cells through the inhibition of cyclin D1.[33] We propose that the changes affecting the structure of the lens capsule in the overexpression mice could affect the ability of epithelial cells to anchor to the capsule, possibly via integrins or cell-surface heparan sulfate proteoglycans, leading to the occurrence of vacuoles and clustering of cells. It is also conceivable that the excess endostatin may lead to alterations in intracellular signaling and thereby to changes in epithelial cell viability.

Western blotting analysis of transgene expression in the skin revealed an ~20-kd fragment. The expression level was highest in line J4 and moderate in line G20, whereas the transgene-derived signal in the K18 line was comparable to the endogenous level. In contrast to the lens, transgene expression in the skin did not lead to obvious defects detectable at the light microscopy level, but ultrastructural analysis did reveal a broadened epidermal BM in lines J4 and G20. More specifically, in both lines the BM was continuous but consistently broadened, the broadening being conspicuous in the J4 skin and more moderate in G20 skin, and in addition there were pearl-like protrusions in some areas of the J4 epidermal BM. When measuring the thicknesses of the epidermal BMs we found that the lamina densa of the epidermal BM in the line was twice as broad in J4 mice and 31% broader in G20 compared with the controls.

We also performed immunoelectron microscopy studies of simultaneous labeling with antibodies specific to the N-terminal and C-terminal domains of type XVIII collagen. The endostatin epitopes were located within the lamina densa at a distance of 46.80 ± 18 nm from the epithelial edge of the lamina densa whereas the N-terminal epitopes were at the BM-stroma interphase at a distance of 87.61 ± 48.61 nm from the edge of the lamina densa. Thus there is a difference between the two epitope signals of ~40 nm, and the results indicate a polarized location of type XVIII collagen molecules in the epidermal BM zone. In the transgenic mice the endostatin signal was stronger but coincided with the localization of the endogenous endostatin domain of type XVIII collagen. Interestingly, the immunosignals for the N-terminal epitope were reduced in the transgenic skin because fewer gold particles were detected in the fields and the signals were often occurring deeper in the dermis when comparing mutant and control samples.

It has been shown that a lack of type XVIII collagen leads to broadening of the epithelial BM of the iris and ciliary body.[18] We show here that overexpression of the endostatin domain similarly led to broadening of the skin BM. We used antibodies against major BM components to test whether this broadening is because of dispersion or compensatory overproduction of some other BM components, but immunostaining of some BM components did not reveal any changes in their expression patterns between the transgenic and wild-type samples in either light or electron microscopy (not shown).

The polarized location of type XVIII collagen molecules, the C-terminal endostatin domain being embedded in the basal lamina and the N-terminal noncollagenous domain occurring at the BM-fibrillar matrix interface, and the apparent displacement of type XVIII collagen molecules to the fibrillar matrix in the event of overexpression of monomeric endostatin, are intriguing findings. It is known that the type XVIII collagen NC1 domain, which contains the endostatin domain in trimeric form, binds the BM proteins laminin-1 and perlecan more strongly than does monomeric endostatin, whereas both bind fibulin-1, fibulin-2, and heparin equally well,[11] and it is thus conceivable that the large amount of transgene-derived endostatin in mice that overexpress this component may compete for binding sites with the full-length type XVIII collagen molecules, leading to their displacement. The broadening of the BMs in the absence of this molecule and the apparent phenocopying of this BM defect when monomeric endostatin is overexpressed in mice synthesizing the full-length type XVIII collagen molecules are suggestive of a molecular explanation for the role of type XVIII collagen. We propose that this collagen, and in particular its trimeric endostatin domain, has a role in binding other BM components together, leading to tightening of the network of BM molecules (Figure 6E). When monomeric endostatin is introduced, it competes with these binding sites, but it is not as efficient as trimeric endostatin in supporting the molecular network. Alternatively, displacement of the full-length type XVIII collagen molecules affects the anchorage of the lamina densa to the dermis. Thus both a lack of type XVIII collagen and overexpression of its endostatin domain could affect the structural integrity of the BMs. Further work is needed to validate this model and to identify the key binding partners. It can also be envisaged that the proposed model may help us to understand the multiple roles that type XVIII collagen appears to have, in supporting BM integrity but also in potentiating the destabiliza-

tion of BMs in the course of their synthesis and in degradation situations associated with increased expression of proteolytic enzymes such as the matrix metalloproteinases, which are known to be able to release monomeric endostatin.[13–15] The functional significance of the endostatin overexpression will be addressed in future studies including studying the effects of the observed BM abnormalities on wound healing and tumor growth.

Acknowledgments

We thank Dr. Naomi Fukai and Dr. Björn Olsen for the *Col18a1*$^{-/-}$ mice; Dr. Kari Alitalo for his contribution to generating the K14 transgenic mice; and Päivi Tuomaala, Anna-Liisa Oikarainen, and Sirpa Kellokumpu for their excellent technical assistance.

References

1. Muragaki Y, Timmons S, Griffith CM, Oh SP, Fadel B, Quertermous T, Olsen BR: Mouse Col18a1 is expressed in a tissue-specific manner as three alternative variants and is localized in basement membrane zones. Proc Natl Acad Sci USA 1995, 92:8763–8767
2. Saarela J, Rehn M, Oikarinen A, Autio-Harmainen H, Pihlajaniemi T: The short and long forms of type XVIII collagen show clear tissue specificities in their expression and location in basement membrane zones in humans. Am J Pathol 1998, 153:611–626
3. Rehn M, Pihlajaniemi T: Identification of three N-terminal ends of type XVIII collagen chains and tissue-specific differences in the expression of the corresponding transcripts. The longest form contains a novel motif homologous to rat and Drosophila frizzled proteins. J Biol Chem 1995, 270:4705–4711
4. Ackley BD, Crew JR, Elamaa H, Pihlajaniemi T, Kuo CJ, Kramer JM: The NC1/endostatin domain of Caenorhabditis elegans type XVIII collagen affects cell migration and axon guidance. J Cell Biol 2001, 152:1219–1232
5. Elamaa H, Peterson J, Pihlajaniemi T, Destrèe O: Cloning of three variants of type XVIII collagen and their expression patterns during Xenopus laevis development. Mech Dev 2002, 114:109–113
6. O'Reilly MS, Boehm T, Shing Y, Fukai N, Vasios G, Lane WS, Flynn E, Birkhead JR, Olsen BR, Folkman J: Endostatin: an endogenous inhibitor of angiogenesis and tumor growth. Cell 1997, 88:277–285
7. Kuo CJ, LaMontagne Jr KR, Garcia-Cardena G, Ackley BD, Kalman D, Park S, Christofferson R, Kamihara J, Ding YH, Lo KM, Gillies S, Folkman J, Mulligan RC, Javaherian K: Oligomerization-dependent regulation of motility and morphogenesis by the collagen XVIII NC1/endostatin domain. J Cell Biol 2001, 152:1233–1246
8. Rehn M, Veikkola T, Kukk-Valdre E, Nakamura H, Ilmonen M, Lombardo C, Pihlajaniemi T, Alitalo K, Vuori K: Interaction of endostatin with integrins implicated in angiogenesis. Proc Natl Acad Sci USA 2001, 98:1024–1029
9. Karumanchi SA, Jha V, Ramchandran R, Karihaloo A, Tsiokas L, Chan B, Dhanabal M, Hanai JI, Venkataraman G, Shriver Z, Keiser N, Kalluri R, Zeng H, Mukhopadhyay D, Chen RL, Lander AD, Hagihara K, Yamaguchi Y, Sasisekharan R, Cantley L, Sukhatme VP: Cell surface glypicans are low-affinity endostatin receptors. Mol Cell 2001, 7:811–822
10. Sasaki T, Fukai N, Mann K, Gohring W, Olsen BR, Timpl R: Structure, function and tissue forms of the C-terminal globular domain of collagen XVIII containing the angiogenesis inhibitor endostatin. EMBO J 1998, 17:4249–4256
11. Sasaki T, Larsson H, Tisi D, Claesson-Welsh L, Hohenester E, Timpl R: Endostatins derived from collagens XV and XVIII differ in structural and binding properties, tissue distribution and anti-angiogenic activity. J Mol Biol 2000, 301:1179–1190
12. Hanai J, Gloy J, Karumanchi SA, Kale S, Tang J, Hu G, Chan B, Ramchandran R, Jha V, Sukhatme VP, Sokol S: Endostatin is a potential inhibitor of Wnt signaling. J Cell Biol 2002, 158:529–539
13. Wen W, Moses MA, Wiederschain D, Arbiser JL, Folkman J: The generation of endostatin is mediated by elastase. Cancer Res 1999, 59:6052–6056
14. Ferreras M, Felbor U, Lenhard T, Olsen BR, Delaisse J: Generation and degradation of human endostatin proteins by various proteinases. FEBS Lett 2000, 486:247–251
15. Felbor U, Dreier L, Bryant RA, Ploegh HL, Olsen BR, Mothes W: Secreted cathepsin L generates endostatin from collagen XVIII. EMBO J 2000, 19:1187–1194
16. Fukai N, Eklund L, Marneros AG, Oh SP, Keene DR, Tamarkin L, Niemelä M, Ilves M, Li E, Pihlajaniemi T, Olsen BR: Lack of collagen XVIII/endostatin results in eye abnormalities. EMBO J 2002, 21:1535–1544
17. Marneros AG, Keene DR, Hansen U, Fukai N, Moulton K, Goletz PL, Moiseyev G, Pawlyk BS, Halfter W, Dong S, Shibata M, Li T, Crouch RK, Bruckner P, Olsen BR: Collagen XVIII/endostatin is essential for vision and retinal pigment epithelial function. EMBO J 2004, 23:89–99
18. Ylikärppä R, Eklund L, Sormunen R, Kontiola AI, Utriainen A, Määttä M, Fukai N, Olsen BR, Pihlajaniemi T: Lack of type XVIII collagen results in anterior ocular defects. FASEB J 2003, 17:2257–2259
19. Marneros AG, Olsen BR: Age-dependent iris abnormalities in collagen XVIII/endostatin deficient mice with similarities to human pigment dispersion syndrome. Invest Ophthalmol Vis Sci 2003, 44:2367–2372
20. Sertie AL, Sossi V, Camargo AA, Zatz M, Brahe C, Passos-Bueno MR: Collagen XVIII, containing an endogenous inhibitor of angiogenesis and tumor growth, plays a critical role in the maintenance of retinal structure and in neural tube closure (Knobloch syndrome). Hum Mol Genet 2000, 9:2051–2058
21. Suzuki OT, Sertie AL, Der Kaloustian VM, Kok F, Carpenter M, Murray J, Czeizel AE, Kliemann SE, Rosemberg S, Monteiro M, Olsen BR, Passos-Bueno MR: Molecular analysis of collagen XVIII reveals novel mutations, presence of a third isoform, and possible genetic heterogeneity in Knobloch syndrome. Am J Hum Genet 2002, 71:1320–1329
22. Lin Y, Zhang S, Rehn M, Itäranta P, Tuukkanen J, Heljasvaara R, Peltoketo H, Pihlajaniemi T, Vainio S: Induced repatterning of type XVIII collagen expression in ureter bud from kidney to lung type: association with sonic hedgehog and ectopic surfactant protein C. Development 2001, 128:1573–1585
23. Vassar R, Rosenberg M, Ross S, Tyner A, Fuchs E: Tissue-specific and differentiation-specific expression of a human K14 keratin gene in transgenic mice. Proc Natl Acad Sci USA 1989, 86:1563–1567
24. Rehn M, Hintikka E, Pihlajaniemi T: Primary structure of the alpha 1 chain of mouse type XVIII collagen, partial structure of the corresponding gene, and comparison of the alpha 1(XVIII) chain with its homologue, the alpha 1(XV) collagen chain. J Biol Chem 1994, 269:13929–13935
25. Kawashima H, Watanabe N, Hirose M, Sun X, Atarashi K, Kimura T, Shikata K, Matsuda M, Ogawa D, Heljasvaara R, Rehn M, Pihlajaniemi T, Miyasaka M: Collagen XVIII, a basement membrane heparan sulfate proteoglycan, interacts with L-selectin and monocyte chemoattractant protein-1. J Biol Chem 2003, 278:13069–13076
26. McAvoy JW, Chamberlain CG, de Iongh RU, Hales AM, Lovicu FJ: Lens development. Eye 1999, 13:425–437
27. Nguyen MM, Potter SJ, Griep AE: Deregulated cell cycle control in lens epithelial cells by expression of inhibitors of tumor suppressor function. Mech Dev 2002, 112:101–113
28. Bassnett S, Missey H, Vucemilo I: Molecular architecture of the lens fiber cell basal membrane complex. J Cell Sci 1999, 112:2155–2165
29. Zampighi GA, Eskandari S, Kreman M: Epithelial organization of the mammalian lens. Exp Eye Res 2000, 71:415–435
30. Sudhakar A, Sugimoto H, Yang C, Lively J, Zeisberg M, Kalluri R: Human tumstatin and human endostatin exhibit distinct antiangiogenic activities mediated by alpha v beta 3 and alpha 5 beta 1 integrins. Proc Natl Acad Sci USA 2003, 100:4766–4771
31. Kreuger J, Matsumoto T, Vanwildemeersch M, Sasaki T, Timpl R, Claesson-Welsh L, Spillmann D, Lindahl U: Role of heparan sulfate domain organization in endostatin inhibition of endothelial cell function. EMBO J 2002, 21:6303–6311
32. Wickström SA, Alitalo K, Keski-Oja J: Endostatin associates with lipid rafts and induces reorganization of the actin cytoskeleton via down-regulation of RhoA activity. J Biol Chem 2003, 278:37895–37901
33. Hanai J, Dhanabal M, Karumanchi SA, Albanese C, Waterman M, Chan B, Ramchandran R, Pestell R, Sukhatme VP: Endostatin causes G1 arrest of endothelial cells through inhibition of cyclin D1. J Biol Chem 2002, 277:16464–16469